

# Direct Measurement of Competing Quantum Effects on the Kinetic Energy of Heavy Water upon Melting

Giovanni Romanelli,<sup>†</sup> Michele Ceriotti,<sup>\*,‡</sup> David E. Manolopoulos,<sup>‡</sup> Claudia Pantalei,<sup>¶,⊥</sup> Roberto Senesi,<sup>\*,†</sup> and Carla Andreani<sup>†</sup>

<sup>†</sup>Dipartimento di Fisica e Centro NAST, Università degli Studi di Roma "Tor Vergata", Via della Ricerca Scientifica 1, 00133 Roma, Italy

<sup>‡</sup>Physical and Theoretical Chemistry Laboratory, University of Oxford, South Parks Road, Oxford OX1 3QZ, United Kingdom

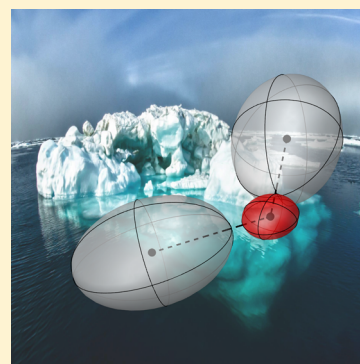
<sup>¶</sup>Laboratoire Léon Brillouin, CEA, Saclay, France

<sup>⊥</sup>Consiglio Nazionale delle Ricerche, CNR-IPCF, Sezione di Messina, Messina, Italy

## S Supporting Information

**ABSTRACT:** Even at room temperature, quantum mechanics plays a major role in determining the quantitative behavior of light nuclei, changing significantly the values of physical properties such as the heat capacity. However, other observables appear to be only weakly affected by nuclear quantum effects (NQE); for instance, the melting temperatures of light and heavy water differ by less than 4 K. Recent theoretical work has attributed this to a competition between intra- and intermolecular NQEs, which can be separated by computing the anisotropy of the quantum kinetic energy tensor. The principal values of this tensor change in opposite directions when ice melts, leading to a very small net quantum mechanical effect on the melting point. This Letter presents the first direct experimental observation of this phenomenon, achieved by measuring the deuterium momentum distributions  $n(\mathbf{p})$  in heavy water and ice using deep inelastic neutron scattering (DINS) and resolving their anisotropy. Results from the experiments, supplemented by a theoretical analysis, show that the anisotropy of the quantum kinetic energy tensor can also be captured for heavier atoms such as oxygen. (The iceberg image in the Table of Contents and Abstract graphics was used with permission of the NOAA's National Ocean Service, 2012 ([http://commons.wikimedia.org/wiki/File:Iceberg\\_-\\_NOAA.jpg](http://commons.wikimedia.org/wiki/File:Iceberg_-_NOAA.jpg))).

**SECTION:** Liquids; Chemical and Dynamical Processes in Solution



The structure and dynamics of liquid water are directly influenced by quantum mechanics, not only in terms of the electronic structure and chemical bonding but also at the level of the nuclear motion. So-called nuclear quantum effects (NQEs) include zero-point energy, tunnelling, isotope effects in the thermodynamic properties, and, what is most relevant to the present work, large deviations from the classical, Maxwell–Boltzmann behavior of both the average nuclear kinetic energy  $\langle E_K \rangle$  and the momentum distribution  $n(\mathbf{p})$ .

Even though NQEs are very large (the zero-point energy content of an O–H stretching vibration is in excess of 200 meV), it is often the case that their net effect on macroscopic properties is relatively small. For instance, the melting temperatures of light and heavy water differ by less than 4 K, and the boiling temperatures differ by just 1 K. Recent theoretical analyses<sup>1,2</sup> have suggested that this could stem from a partial cancellation between quantum effects in the intra- and intermolecular components of the hydrogen bond, so that the net effect is small even if the individual contributions are large. In particular, the competition between quantum effects can be seen very clearly when decomposing the changes in the

quantum kinetic energy of protons and deuterons along different molecular axes.<sup>3,4</sup>

The mechanism that underlies the competition between changes in the different components of the quantum kinetic energy can be understood by considering as an analogy a two-level quantum system with an environment-dependent off-diagonal coupling  $\beta$ . A small change in the coupling  $\Delta\beta$ , arising from a phase transition or some other change in the environment of the system, will shift its eigenvalues by the same amount proportional to  $\Delta\beta$ , but in opposite directions. Even though this picture is clearly oversimplified, it is consistent with a diabatic state model of the hydrogen bond,<sup>5</sup> it demonstrates that the notion of competing quantum effects is nothing exotic, and explains why it returns in many circumstances in the study of water and other hydrogen-bonded systems.

Competing quantum effects have in fact been identified in a diverse variety of simulations,<sup>1–4</sup> and it seems entirely plausible

Received: July 20, 2013

Accepted: September 6, 2013

Published: September 6, 2013

that they are at the root of the explanation for why many of the properties of water depend only weakly on isotopic composition. As discussed in the Supporting Information (SI), the change of many thermodynamic properties upon isotopic substitution can be related to changes in the quantum kinetic energy.<sup>3,6</sup> Under a few simplifying assumptions, one can, for instance, relate the change in the quantum kinetic energy of the D atoms when heavy water melts,  $\Delta_{\text{fus}}E_{\text{K}}(m_{\text{D}}, T_{\text{fus}}(m_{\text{D}}))$ , to macroscopic thermodynamic properties such as the entropy of melting of light water,  $\Delta_{\text{fus}}S(m_{\text{H}})$ , and the change in the melting temperature upon isotopic substitution

$$\Delta_{\text{fus}}E_{\text{K}}(m_{\text{D}}, T_{\text{fus}}(m_{\text{D}})) \approx \frac{\Delta_{\text{fus}}S(m_{\text{H}})}{2(\sqrt{m_{\text{D}}/m_{\text{H}}} - 1)} [T_{\text{fus}}(m_{\text{H}}) - T_{\text{fus}}(m_{\text{D}})] \quad (1)$$

Equation 1 predicts a change in kinetic energy per D atom of  $\Delta_{\text{fus}}E_{\text{K}} = -0.5$  meV. This is a tiny value, less than 0.5% of the total kinetic energy of the D atoms at room temperature. A direct experimental investigation of the competing quantum effects at play here should reveal whether this happens because of a cancellation or because the environment of a D atom changes very little upon melting.

Deep inelastic neutron scattering (DINS), or neutron Compton scattering (NCS) at high momentum and energy transfers ( $\hbar q$  and  $\hbar\omega$ , respectively), is an experimental technique that is particularly well suited to probe the quantum behavior of atomic nuclei, by directly measuring  $n(\mathbf{p})$ .<sup>7–9</sup> The results from DINS experiments have stimulated the development of improved theoretical methods for evaluating the proton momentum distribution,<sup>10–13</sup> as well as their application to benchmark systems, with a close interplay between theory and experiment.<sup>14,15</sup> One can infer the anisotropy of the particle momentum distribution from DINS experiments even in cases when only the spherically averaged  $n(p)$  is available. In water, this provides insight into the local environment of the proton and can help elucidate the nature of hydrogen bonding,<sup>7,16,17</sup> the structure of hydration shells, and the effects of confinement.<sup>18–20</sup> Indeed this information can be seen as the direct experimental counterpart of the decomposition of the quantum kinetic energy along molecular axes, which has been used so successfully to unravel competing quantum effects in simulations.<sup>3,4,13</sup>

The focus of DINS studies has recently broadened to consider also heavier atoms,<sup>13,21,22</sup> which, although challenging because of their less-pronounced quantum nature, promise a more comprehensive picture of the underlying physics. Theoretical calculations<sup>23,24</sup> demonstrate a sizable excess of kinetic energy for the oxygen atoms in ice, relative to the classical value. This kinetic energy excess shows a clear dependence on the chemical environment<sup>25</sup> and on the microscopic structure. A direct, accurate measurement of the kinetic energy of the oxygen atoms could, for instance, shed light on recent findings that indicate an increased localization of the oxygen in heavy water compared to that in light water, as evidenced by a 10% overstructuring in the heavy water  $g_{\text{OO}}(r)$  radial distribution function.<sup>26</sup>

At present, the only instrumentation suitable to perform measurements of  $n(\mathbf{p})$  in condensed matter systems is the VESUVIO spectrometer, which operates on a dedicated beamline at the pulsed neutron source ISIS (Rutherford Appleton Laboratory, U.K.).<sup>9,27</sup> The instrument uses neutrons with incident energies in the range of 1–800 eV and relies on

the fact that, at sufficiently high momentum transfers, any scattering process can be described within the impulse approximation (IA).<sup>28</sup> This implies that the neutron scatters from a single atom, with conservation of the total kinetic energy and momentum of the neutron and the atom.<sup>29</sup> In the IA regime the inelastic neutron scattering cross section is related in a simple way to  $n(\mathbf{p})$ . The neutron scattering function  $S_{\text{IA}}(\mathbf{q}, \omega)$  is

$$\frac{\hbar q}{m} S_{\text{IA}}(\mathbf{q}, \omega) = J_{\text{IA}}(y, \hat{\mathbf{q}}) = \int n(\mathbf{p}) \delta(y - \mathbf{p} \cdot \hat{\mathbf{q}}) d\mathbf{p} \quad (2)$$

where  $(\mathbf{q}, \omega)$  are the wave vector and energy transfers,  $m$  is the mass of the atom being struck,  $y = (m/\hbar q)[\omega - (\hbar q^2/2m)]$  is the particle momentum along the  $q$  direction, and  $J_{\text{IA}}(y, \hat{\mathbf{q}})$  is the neutron Compton profile (NCP) (for consistency with previous literature and ease of notation we write the momentum as a wave vector).

When the sample is isotropic, the particle momentum distribution only depends on the modulus of  $\mathbf{p}$ , and the  $\hat{\mathbf{q}}$  direction is immaterial; therefore, the NCP is simply  $J_{\text{IA}}(y) = 2\pi \int_{|\mathbf{p}|} p n(p) dp$ . This ideal peak profile is broadened by finite- $q$  correction terms  $\Delta J(y, q)$ , as discussed in the SI,<sup>30</sup> and by convolution with the instrumental resolution function  $R(y, q)$ ; therefore, the experimental NCP,  $F(y, q)$ , is

$$F(y, q) = [J_{\text{IA}}(y) + \Delta J(y, q)] \otimes R(y, q) \quad (3)$$

One reasonable (and also insightful) way to extract the physical information content from the experimental  $F(y, q)$  profile is to assume that the underlying  $n(p)$  arises from the spherical average of an anisotropic Gaussian distribution<sup>15,23,31,32</sup>

$$4\pi p^2 n(p) = \int \frac{\delta(p - |\mathbf{p}|)}{\sqrt{8\pi^3 \sigma_x \sigma_y \sigma_z}} \exp\left(-\frac{p_x^2}{2\sigma_x^2} - \frac{p_y^2}{2\sigma_y^2} - \frac{p_z^2}{2\sigma_z^2}\right) d^3\mathbf{p} \quad (4)$$

This expression involves three parameters, the variances  $\sigma_\alpha^2$  for  $\alpha = x, y, z$ , which are related to three effective principal frequencies  $\omega_\alpha$  by  $\sigma_\alpha^2 = (m\omega_\alpha/2\hbar) \coth(\beta\hbar\omega_\alpha/2)$ , or to the three components of the quantum kinetic energy by  $\langle E_\alpha \rangle = \hbar^2\sigma_\alpha^2/2m$ . In the present study, this approach has been used to interpret DINS data acquired on heavy water in the solid at 274 K and in the liquid at 280 and 300 K.

To complement this experimental study, we have also performed some new ab initio computer simulations of heavy water and ice, using the same density functional theory (DFT) framework<sup>33–36</sup> as that described in ref 13. Tests with different basis sets and the inclusion of dispersion corrections produced no qualitative changes in the results. NQEs were incorporated using the PIGLET technique,<sup>13</sup> which combines the path integral formalism<sup>37,38</sup> with a correlated-noise Langevin equation,<sup>12,13</sup> thereby enabling fully converged results for room-temperature water to be obtained with as few as six path integral beads.

The conventional way to extract the particle momentum distribution from the path integral formalism involves opening the path and is computationally very demanding.<sup>14</sup> A simpler alternative is to assume that the momentum distribution can be modeled as a multivariate Gaussian as in eq 4 and to use the eigenvalues of the quantum kinetic energy tensor  $\hbar^2\langle p_\alpha p_\beta \rangle/2m$  to estimate the principal components of this distribution. The only difficulty here lies in the fact that in the liquid, the orientations of the water molecules change with time; therefore,

one cannot simply average the centroid virial estimator to obtain the anisotropic kinetic energy tensor.

Here, we compare two different ways around this difficulty. One is to perform a running average of the kinetic energy estimator,<sup>13</sup> the so-called “transient anisotropic Gaussian” (TAG) approximation. For this, we used a triangular averaging window of 100 fs, which has previously been shown to give converged results for light water.<sup>13</sup> Another possibility is to assume that the principal axes of the kinetic energy tensor will have a fixed orientation relative to the molecular geometry. One can then perform a mean-square displacement (MSD) alignment of the instantaneous configuration of each water molecule to a reference structure, rotating the kinetic energy estimator into the molecular reference frame and computing its average and its eigenvalues.<sup>3,4</sup> We will show that the two approaches give results that are consistent with one another and that they enable a direct comparison with the DINS experiment.

Figure 1 reports examples of the experimental detector-averaged NCP for D and O,  $\bar{F}(y,q)$ , together with the best fits

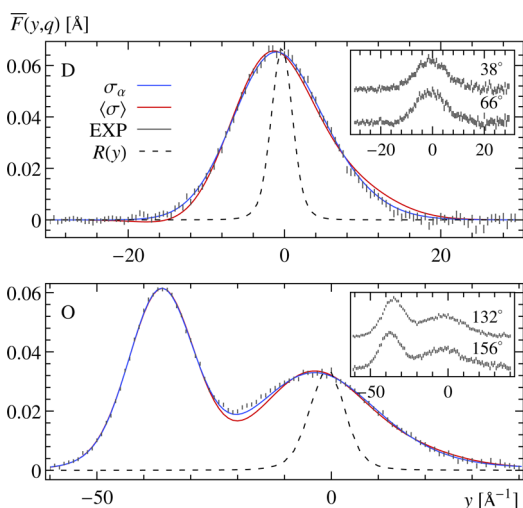


**Figure 1.** Experimental NCS profiles for heavy ice at  $T = 274$  K. The two panels report the detector-averaged NCS for D (upper panel) and O (lower panel). Best fits using simple Gaussian (red line) and spherically averaged multivariate Gaussian (blue line) approximations to the momentum distribution are also reported. In the case of the O profiles, the peak at  $y = -40 \text{ \AA}^{-1}$  is due to the contribution from the Cu sample container. The instrumental resolution is reported as a black dotted line, and the insets show examples of the raw data from two individual detectors for D and from two groups of detectors at the same scattering angles for O.

obtained with an isotropic and a multivariate Gaussian ansatz for  $n(p)$ . The angle-averaged  $\bar{F}(y,q)$  is obtained by averaging over the detectors in the range of  $32\text{--}66^\circ$  for D and those between  $130$  and  $163^\circ$  for O. Data were not symmetrized. This figure provides a graphical representation of the overall quality of both the data and the fit (see also the SI). Clearly, the multivariate Gaussian profile provides a better fit to the experimental data than an isotropic Gaussian.

In the upper panels of Figure 2, we compare the experimental and theoretical  $n(p)$ 's for liquid  $\text{D}_2\text{O}$  at 300 K. There is a near-perfect agreement between theory and experiment in the case of D. The discrepancy is larger in the case of O but comparable with the error bar and much smaller

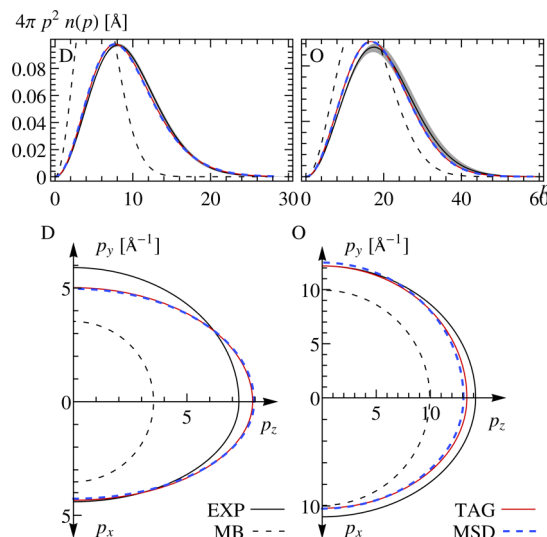


**Figure 2.** Comparison of the momentum distributions of O and D in liquid  $\text{D}_2\text{O}$  at 300 K, as obtained from the analysis of DINS experimental data and from two different analyses of the ab initio PIGLET simulations. In all plots, the continuous black curve corresponds to the experimental data, the red curve to a TAG analysis, and the blue curve to a MSD analysis of the simulation data. The dashed line corresponds to what would be expected if  $n(p)$  were just a classical, Maxwell–Boltzmann distribution. The upper panels show the spherically averaged  $n(p)$  (the shaded area around the experimental curve represents the confidence interval), while the lower panels contain a graphical representation of the anisotropy. The curves correspond to isosurfaces of the  $n(\mathbf{p})$  cut along the  $xz$  and  $yz$  planes. The contour line is chosen in such a way that the intercepts on the axes are the values of  $\sigma_{\alpha}$ .

than the deviation from a classical, Maxwell–Boltzmann distribution.

The lower panels show that the discrepancy between theory and experiment is more pronounced when one focuses on the anisotropy of the distribution. The TAG and MSD approximations are consistent with each other, as discussed in more detail in the SI. It is interesting that, despite the noticeable differences in the individual values of  $\langle E_{\alpha} \rangle$ , the theoretical and experimental  $n(p)$ 's for D are almost indistinguishable. However, the theoretical and experimental  $n(p)$ 's for O, which involve a larger discrepancy in the total  $\langle E_{\mathbf{K}} \rangle$  but smaller discrepancies in the individual components, show a more evident difference. Because of the averaging in eq 4, the computed  $n(p)$  depends only weakly on how the kinetic energy components are distributed, but in a more pronounced way on the total kinetic energy.

The relative insensitivity of  $n(p)$  to the partitioning of  $\langle E_{\mathbf{K}} \rangle$  into three principal components justifies the use of either the TAG or the MSD approach to estimate the anisotropy of the kinetic energy tensor. However, this insensitivity also means that extracting the anisotropy from the spherically averaged  $n(p)$  is an ill-conditioned problem. For this reason, the analysis of the experimental data typically yields larger relative errors in the individual components of the kinetic energy than in the total.

Bearing this in mind, let us now discuss how DINS can provide a direct verification of the concept of competing quantum effects in water. Table 1 collects all of the present experimental and theoretical results together in a compact form. The agreement between the total deuterium kinetic

**Table 1. Comparison between Theoretical and Experimental Components of the Quantum Kinetic Energy for D and O in Heavy Water, At Different Temperatures<sup>a</sup>**

	D [exp]	D [TAG/MSD]	O [exp]	O [TAG/MSD]
D <sub>2</sub> O, T = 300 K, liquid				$\langle E_{\text{COM}} \rangle = 42.1$
$\langle E_x \rangle$	20.1 ± 1.1	19.5/18.9	15.8 ± 1.7	13.6/13.7
$\langle E_y \rangle$	36.1 ± 2.3	26.1/25.6	19.5 ± 1.3	19.4/20.4
$\langle E_z \rangle$	55.1 ± 2.3	64.6/65.7	26.3 ± 1.5	23.4/22.3
$\langle E_K \rangle$	111.3 ± 3	110.2	61.6 ± 3.1	56.4
D <sub>2</sub> O, T = 280 K, liquid				$\langle E_{\text{COM}} \rangle = 39.5$
$\langle E_x \rangle$	18.8 ± 1.1	19.4/18.9	16.0 ± 2.3	13.6/13.7
$\langle E_y \rangle$	38.6 ± 2.5	25.7/25.2	21.0 ± 0.6	19.2/20.2
$\langle E_z \rangle$	54.2 ± 2.4	63.6/64.6	24.1 ± 2.1	23.2/22.2
$\langle E_K \rangle$	111.6 ± 2	108.7	61.1 ± 3.1	56.1
D <sub>2</sub> O, T = 274 K, liquid				$\langle E_{\text{COM}} \rangle = 38.9$
$\langle E_x \rangle$		19.3/19.0		13.4/13.5
$\langle E_y \rangle$		25.8/25.3		19.1/20.1
$\langle E_z \rangle$		63.2/64.1		23.1/22.0
$\langle E_K \rangle$		108.3		55.6
D <sub>2</sub> O, T = 274 K, solid				$\langle E_{\text{COM}} \rangle = 39.2$
$\langle E_x \rangle$	22.5 ± 1.8	20.1/19.8	16.1 ± 2.3	13.7/13.8
$\langle E_y \rangle$	37.4 ± 2.5	26.3/25.9	20.1 ± 1.6	19.0/19.9
$\langle E_z \rangle$	48.1 ± 3.4	61.9/62.4	24.2 ± 1.4	23.0/21.9
$\langle E_K \rangle$	108.0 ± 2	108.3	60.4 ± 4	55.7

<sup>a</sup>All values are in meV, and the theoretical results have a statistical error bar smaller than 0.1 meV. We also report the computed center-of-mass mean kinetic energy  $\langle E_{\text{COM}} \rangle$  of the D<sub>2</sub>O molecules.

energy obtained by DINS and that by simulation is almost perfect. The change in kinetic energy between the liquid at 300 and 280 K is much smaller than the drop in classical thermal energy, which is consistent with the deuteron being almost completely frozen in its vibrational ground state. There is also agreement with previous experiments at  $T = 292$  K within their (much larger) error bar.<sup>39</sup>

The most interesting results in Table 1 concern the behavior of the momentum distribution in heavy water upon freezing. When going from the liquid to the solid, the DINS data show substantial changes in  $\langle E_x \rangle_{\text{D}}$  (associated with motion perpendicular to the plane of the water molecule<sup>3,13</sup>) and in  $\langle E_z \rangle_{\text{D}}$  (associated with motion parallel to the covalent O–H bond). However, the two components change in opposite directions, leading to a much smaller change in the total kinetic energy, which is not statistically significant given the experimental error bars. The increase in  $\langle E_x \rangle_{\text{D}}$  is a signature of the more hindered librations in the solid phase, while the decrease of  $\langle E_z \rangle_{\text{D}}$  signals a weakening of the covalent bond, which is consistent with the red shift of the stretching peak observed in the vibrational spectroscopy of ice.<sup>40</sup> These observations therefore provide a direct experimental verification of the competition between quantum effects resolved along different molecular axes.

Simulations predict the same qualitative effect on the different components of  $\langle E_K \rangle$ ;  $\langle E_z \rangle_{\text{D}}$  decreases upon freezing, but  $\langle E_x \rangle_{\text{D}}$  increases, leaving almost no change in the total kinetic energy. Performing simulations of the liquid at 280 K and of both the liquid and the solid at 274 K allows us to infer that these effects are due to the phase transition and not the 6 K temperature drop. Note that our simulations show no sign of an increase in quantum kinetic energy upon supercooling, confirming previous theoretical results for light water.<sup>6</sup> The present experiments were deliberately performed well into the

stable solid and liquid phases of heavy water in order to focus on the experimental signature of competing quantum effects upon melting without interference from the more controversial effects that have been observed in DINS measurements on supercooled water.<sup>39,41</sup>

While experiment and theory agree on the qualitative observation of a competition between quantum effects upon melting, there are quantitative discrepancies that deserve further comment. For one thing, our DFT results predict  $\Delta_{\text{fus}} E_K \approx 0$ , whereas simple thermodynamic arguments predict  $\Delta_{\text{fus}} E_K \approx -0.5$  meV (see eq 1). As discussed in the SI, a simple, empirical water model<sup>1</sup> yields predictions that are in agreement with the macroscopic thermodynamic data, which is perhaps unsurprising given that this empirical model accurately describes the change in melting temperature upon isotope substitution.<sup>42</sup> While it is remarkable that an ab initio calculation can get so close to the correct result, it is clear that DFT has not yet reached the level of accuracy necessary to obtain a quantitative description of isotope effects. The DINS experiments also have not reached the exquisite level of accuracy that is necessary to discern such a minute change in the total kinetic energy. Currently, the overall sensitivity of DINS measurements allows one to infer values for proton  $\langle E_K \rangle$  within 2 meV uncertainty<sup>43</sup> and similar if not higher uncertainty for the heavier masses, D and O. Although changes on the order of 0.5 meV are beyond the current sensitivity of the instrument, we have demonstrated that one can nevertheless gain insight into the competition of effects that leads to a small kinetic energy change by resolving the anisotropy of the kinetic energy tensor. The quantitative differences between DINS and PIGLET on the individual components of the kinetic energy, however, indicate that at present, this insight is only qualitative.

Table 1 also presents the results for the oxygen momentum distribution. While there is good qualitative agreement between theory and experiment, we observe a discrepancy of almost 10% in the total kinetic energy, which may stem from shortcomings of the modeling or from the analysis of the experimental data, which is made harder by the weaker signal given by oxygen and by the partial overlap between the  $F(y, q)$  peak of the O and that of the Cu can. Nevertheless, the analysis captures even the comparatively weak anisotropy of the oxygen atom kinetic energy, demonstrating how promising it is to extend DINS to heavy atoms. We anticipate that analysis,<sup>44</sup> software, and instrument upgrades planned on VESUVIO in the near future will enable a greater precision in the simultaneous measurement of light and heavy atoms, enabling one to access quantitative as well as qualitative information on the particle momentum distribution.

## ■ ASSOCIATED CONTENT

### 📄 Supporting Information

Additional details on the relation between the change in kinetic energy upon melting and macroscopic thermodynamic observables, on the analysis of the experimental data, on the technical aspects of the simulations, and on the results obtained with an empirical force field. This material is available free of charge via the Internet at <http://pubs.acs.org>.

## ■ AUTHOR INFORMATION

### Corresponding Authors

\*E-mail: [michele.cerriotti@chem.ox.ac.uk](mailto:michele.cerriotti@chem.ox.ac.uk) (M.C.).

\*E-mail: [roberto.senesi@uniroma2.it](mailto:roberto.senesi@uniroma2.it) (R.S.).

## Notes

The authors declare no competing financial interest.

## ■ ACKNOWLEDGMENTS

This work was partially supported within the CNR-STFC Agreement No. 06/20018 concerning collaboration in scientific research at the spallation neutron source ISIS. C.A. and R.S. acknowledge the support of META (Materials Enhancement for Technological Applications) Marie Curie Actions, People, FP7, PIRSES-GA-2010–269182. M.C. acknowledges funding from the EU Marie Curie IEF No. PIEFGA-2010-272402 and computer time from CSCS (Project ID s388). D.E.M. acknowledges funding from the Wolfson Foundation and the Royal Society.

## ■ REFERENCES

- (1) Habershon, S.; Markland, T. E.; Manolopoulos, D. E. Competing Quantum Effects in the Dynamics of a Flexible Water Model. *J. Chem. Phys.* **2009**, *131*, 24501.
- (2) Li, X. Z.; Walker, B.; Michaelides, A. Quantum Nature of the Hydrogen Bond. *Proc. Natl. Acad. Sci. U.S.A.* **2011**, *108*, 6369.
- (3) Markland, T. E.; Berne, B. J. Unraveling Quantum Mechanical Effects in Water Using Isotopic Fractionation. *Proc. Natl. Acad. Sci. U.S.A.* **2012**, *109*, 7988–7991.
- (4) Liu, J.; Andino, R. S.; Miller, C. M.; Chen, X.; Wilkins, D. M.; Ceriotti, M.; Manolopoulos, D. E. A Surface-Specific Isotope Effect in Mixtures of Light and Heavy Water. *J. Phys. Chem. C* **2013**, *117*, 2944–2951.
- (5) McKenzie, R. H. A Diabatic State Model for Donor-Hydrogen Vibrational Frequency Shifts in Hydrogen Bonded Complexes. *Chem. Phys. Lett.* **2012**, *535*, 196–200.
- (6) Ramírez, R.; Herrero, C. Kinetic Energy of Protons in Ice Ih and Water: A Path Integral Study. *Phys. Rev. B* **2011**, *84*, 064130.
- (7) Andreani, C.; Colognesi, D.; Mayers, J.; Reiter, G. F.; Senesi, R. Measurement of Momentum Distribution of Light Atoms and Molecules in Condensed Matter Systems Using Inelastic Neutron Scattering. *Adv. Phys.* **2005**, *54*, 377–469.
- (8) Pietropaolo, A.; Senesi, R. Electron Volt Neutron Spectrometers. *Phys. Rep.* **2011**, *508*, 45–90.
- (9) Mayers, J.; Reiter, G. The VESUVIO Electron Volt Neutron Spectrometer. *Meas. Sci. Technol.* **2012**, *23*, 045902.
- (10) Ceriotti, M.; Bussi, G.; Parrinello, M. Nuclear Quantum Effects in Solids Using a Colored-Noise Thermostat. *Phys. Rev. Lett.* **2009**, *103*, 30603.
- (11) Lin, L.; Morrone, J. A.; Car, R.; Parrinello, M. Displaced Path Integral Formulation for the Momentum Distribution of Quantum Particles. *Phys. Rev. Lett.* **2010**, *105*, 110602.
- (12) Ceriotti, M.; Manolopoulos, D. E.; Parrinello, M. Accelerating the Convergence of Path Integral Dynamics with a Generalized Langevin Equation. *J. Chem. Phys.* **2011**, *134*, 84104.
- (13) Ceriotti, M.; Manolopoulos, D. E. Efficient First-Principles Calculation of the Quantum Kinetic Energy and Momentum Distribution of Nuclei. *Phys. Rev. Lett.* **2012**, *109*, 100604.
- (14) Morrone, J. A.; Car, R. Nuclear Quantum Effects in Water. *Phys. Rev. Lett.* **2008**, *101*, 17801.
- (15) Ceriotti, M.; Miceli, G.; Pietropaolo, A.; Colognesi, D.; Nale, A.; Catti, M.; Bernasconi, M.; Parrinello, M. Nuclear Quantum Effects in Ab Initio Dynamics: Theory and Experiments for Lithium Imide. *Phys. Rev. B* **2010**, *82*, 174306.
- (16) Reiter, G.; Li, J. C.; Mayers, J.; Abdul-Redah, T.; Platzman, P. The Proton Momentum Distribution in Water and Ice. *Braz. J. Phys.* **2004**, *34*, 142–147.
- (17) Pietropaolo, A.; Senesi, R.; Andreani, C.; Mayers, J. Quantum Effects in Water: Proton Kinetic Energy Maxima in Stable and Supercooled Liquid. *Braz. J. Phys.* **2009**, *39*, 318–321.
- (18) Pantalei, C.; Senesi, R.; Andreani, C.; Sozzani, P.; Comotti, A.; Bracco, S.; Beretta, M.; Sokol, P. E.; Reiter, G. Interaction of Single Water Molecules with Silanols in Mesoporous Silica. *Phys. Chem. Chem. Phys.* **2011**, *13*, 6022.
- (19) Senesi, R.; Pietropaolo, A.; Bocedi, A.; Pagnotta, S. E.; Bruni, F. Proton Momentum Distribution in a Protein Hydration Shell. *Phys. Rev. Lett.* **2007**, *98*, 138102.
- (20) Reiter, G. F.; Senesi, R.; Mayers, J. Changes in the Zero-Point Energy of the Protons as the Source of the Binding Energy of Water to A-Phase DNA. *Phys. Rev. Lett.* **2010**, *105*, 148101.
- (21) Krzystyniak, M.; Fernandez-Alonso, F. Ab Initio Nuclear Momentum Distributions in Lithium Hydride: Assessing Nonadiabatic Effects. *Phys. Rev. B* **2011**, *83*, 134305.
- (22) Seel, A. G.; Ceriotti, M.; Edwards, P. P.; Mayers, J. Simultaneous Measurement of Lithium and Fluorine Momentum in 7LiF. *J. Phys. Condens. Matter* **2012**, *24*, 365401.
- (23) Lin, L.; Morrone, J. A.; Car, R.; Parrinello, M. Momentum Distribution, Vibrational Dynamics, and the Potential of Mean Force in Ice. *Phys. Rev. B* **2011**, *83*, 220302.
- (24) Herrero, C. P.; Ramírez, R. Isotope Effects in Ice Ih: A Path-Integral Simulation. *J. Chem. Phys.* **2011**, *134*, 094510.
- (25) Seel, A. G.; Sartbaeva, A.; Mayers, J.; Ramirez-Cuesta, A. J.; Edwards, P. P. Neutron Compton Scattering Investigation of Sodium Hydride: From Bulk Material to Encapsulated Nanoparticles in Amorphous Silica Gel. *J. Chem. Phys.* **2011**, *134*, 114511.
- (26) Soper, A. K.; Benmore, C. J. Quantum Differences between Heavy and Light Water. *Phys. Rev. Lett.* **2008**, *101*, 065502.
- (27) Senesi, R.; Andreani, C.; Bowden, Z.; Colognesi, D.; Degiorgi, E.; Fielding, A. L.; Mayers, J.; Nardone, M.; Norris, J.; Praitano, M.; Rhodes, N. J.; Stirling, W. G.; Tomkinson, J.; Uden, C. VESUVIO: A Novel Instrument for Performing Spectroscopic Studies in Condensed Matter with eV Neutrons at the ISIS Facility. *Physica B* **2000**, *276*, 200–201.
- (28) West, G. B. Electron Scattering from Atoms, Nuclei and Nucleons. *Phys. Rep.* **1975**, *18*, 263–323.
- (29) Gunn, J. M. F.; Andreani, C.; Mayers, J. A New Approach to Impulsive Neutron Scattering. *J. Phys. C* **1986**, *19*, L835–L840.
- (30) Sears, V. F. Scaling and Final-State Interactions in Deep-Inelastic Neutron Scattering. *Phys. Rev. B* **1984**, *30*, 44–51.
- (31) Andreani, C.; Degiorgi, E.; Senesi, R.; Cilloco, F.; Colognesi, D.; Mayers, J.; Nardone, M.; Pace, E. Single Particle Dynamics in Fluid and Solid Hydrogen Sulphide: An Inelastic Neutron Scattering Study. *J. Chem. Phys.* **2001**, *114*, 387–398.
- (32) Flammini, D.; Pietropaolo, A.; Senesi, R.; Andreani, C.; McBride, F.; Hodgson, A.; Adams, M. A.; Lin, L.; Car, R. Spherical Momentum Distribution of the Protons in Hexagonal Ice from Modeling of Inelastic Neutron Scattering Data. *J. Chem. Phys.* **2012**, *136*, 024504.
- (33) Lee, C.; Yang, W.; Parr, R. G. Development of the Colle–Salvetti Correlation-Energy Formula into a Functional of the Electron Density. *Phys. Rev. B* **1988**, *37*, 785.
- (34) Becke, A. D. Density-Functional Exchange–Energy Approximation with Correct Asymptotic Behavior. *Phys. Rev. A* **1988**, *38*, 3098.
- (35) Goedecker, S.; Teter, M.; Hutter, J. Separable Dual-Space Gaussian Pseudopotentials. *Phys. Rev. B* **1996**, *54*, 1703–1710.
- (36) VandeVondele, J.; Krack, M.; Mohamed, F.; Parrinello, M.; Chassaing, T.; Hutter, J. Quickstep: Fast and Accurate Density Functional Calculations Using a Mixed Gaussian and Plane Waves Approach. *Comput. Phys. Commun.* **2005**, *167*, 103–128.
- (37) Feynman, R. P.; Hibbs, A. R. *Quantum Mechanics and Path Integrals*; McGraw-Hill: New York, 1964.
- (38) Ceperley, D. M. Path Integrals in the Theory of Condensed Helium. *Rev. Mod. Phys.* **1995**, *67*, 279–355.
- (39) Giuliani, A.; Bruni, F.; Ricci, M.; Adams, M. Isotope Quantum Effects on the Water Proton Mean Kinetic Energy. *Phys. Rev. Lett.* **2011**, *106*, 255502.
- (40) Eisenberg, D.; Kauzmann, W. *The Structure and Properties of Water*; Oxford University Press: Oxford, U.K., 1968.

(41) Pietropaolo, A.; Senesi, R.; Andreani, C.; Botti, A.; Ricci, M. A.; Bruni, F. Excess of Proton Mean Kinetic Energy in Supercooled Water. *Phys. Rev. Lett.* **2008**, *100*, 127802.

(42) Ramírez, R.; Herrero, C. P. Quantum Path Integral Simulation of Isotope Effects in the Melting Temperature of Ice Ih. *J. Chem. Phys.* **2010**, *133*, 144511.

(43) Flammini, D.; Pietropaolo, A.; Senesi, R.; Andreani, C.; McBride, F.; Hodgson, A.; Adams, M.; Lin, L.; Car, R. Spherical Momentum Distribution of the Protons in Hexagonal Ice from Modeling of Inelastic Neutron Scattering Data. *J. Chem. Phys.* **2012**, *136*, 024504.

(44) Blostein, J.; Dawidowski, J.; Granada, J. Formalism for Obtaining Nuclear Momentum Distributions by the Deep Inelastic Neutron Scattering Technique. *Phys. Rev. B* **2005**, *71*, 054105.